Characterization of a 90° Microstrip Bend with Arbitrary Miter via the Time-Domain Finite Difference Method

JOHN MOORE, STUDENT MEMBER, IEEE, AND HAO LING, MEMBER, IEEE

Abstract—A 90° microstrip bend with an arbitrary miter is characterized using the finite difference time-domain (FDTD) method. To simplify computations, the microstrip structure is enclosed by four electric walls; thus radiation effects are neglected. Time histories generated by FDTD are Fourier-transformed to yield broad-band S parameters of the microstrip bend. A miter is introduced to improve the transmission characteristics of the bend, and an optimal miter length is found such that the reflection from the microstrip bend over a broad frequency range is minimized.

I. Introduction

THE FINITE difference time-domain (FDTD) method [1], [2] has become recognized as a useful tool for analyzing complicated wave interactions. The versatility of the FDTD method allows it to analyze microstrip line and microstrip discontinuities. Gwarek has developed a method for two-dimensional planar circuit analysis with the FDTD method [3], [4]. Zhang and Mei have computed the dispersive characteristics of microstrip [5] as well as the scattering parameters for the microstrip cross junction, tee junction, step in width, and gap via the FDTD method [6]. This paper focuses on the full-wave analysis of the microstrip right-angle bend. The microstrip bend has been studied extensively in the literature by such approximate methods as quasi-static analysis [7] and the planar waveguide model [8]–[11]. Recently, a qualitative study of wave propagation through the microstrip bend was reported by Yoshida and Fukai [12] using the transmission-line matrix method. In this paper, the time history of a short pulse as it propagates through a microstrip bend is simulated using the FDTD algorithm. Quantitative frequency-domain information contained in the time-domain data is extracted via the Fourier transform.

Computer memory constraints dictate that the computation domain of the FDTD be of finite size. In order to simulate open structures, various localized absorbing boundary conditions have been employed to truncate the FDTD grid [13], [14]. However, for dispersive structures such as the microstrip line, noise from the imperfect absorbing condition can give rise to significant degradation in the frequency-domain data. The FDTD method used in this paper does not employ absorbing conditions. Instead, the microstrip structure is enclosed by electric walls located far enough away from the strip to not seriously affect the field distributions near the strip. This electric wall assumption neglects radiation effects which are reported to be small for the open microstrip bend [15]. The FDTD grid is kept large enough in the direction of propagation so that an expanding wave never reflects off the edge of the grid.

Cutting a miter into a microstrip or waveguide bend is a well-known method for reducing reflections caused by sharp corners in waveguide bends [16]. Campbell and Jones [17] studied the 90° parallel-plate waveguide bend with a 45° miter of arbitrary length and showed that there exists an optimal cut size that minimizes reflections. Later, Douville and James [15] performed experiments on microstrip and constructed an empirical formula that relates the optimal miter to the width-to-height ratio of the strip. Results obtained by the FDTD method for the optimal cut size of the enclosed microstrip bend are also presented in this paper for a range of width-to-height ratios. They confirm Douville and James's earlier experimental results.

II. Time-Domain Simulation

Fig. 1(a) shows the top view of the 90° microstrip bend with a 45° miter to be analyzed. The distance from the inner corner of the bend to the outer corner, assuming no cut, is denoted d, and x is the distance from the inner corner of the bend to the midpoint of the cut. The amount of cut is the quantity $m = x/d$, where $m = 0$ indicates a bend with no cut and $m = 1$ indicates a cut large enough to barely separate the two sections of microstrip from the bend. The microstrip is enclosed on four sides by electric walls as shown in Fig. 1(b). The width, a, and height, b, of this box must be large enough to not disturb the field distributions near the strip.

Manuscript received May 25, 1989; revised October 2, 1989. This work was supported by the National Science Foundation under Grant ECS-8657524 and by the Texas Advanced Technology Program.

The authors are with the Department of Electrical and Computer Engineering, University of Texas at Austin, Austin, TX 78712.

IEEE Log Number 8933714.

0018-9480/90/0400-0405$01.00 ©1990 IEEE

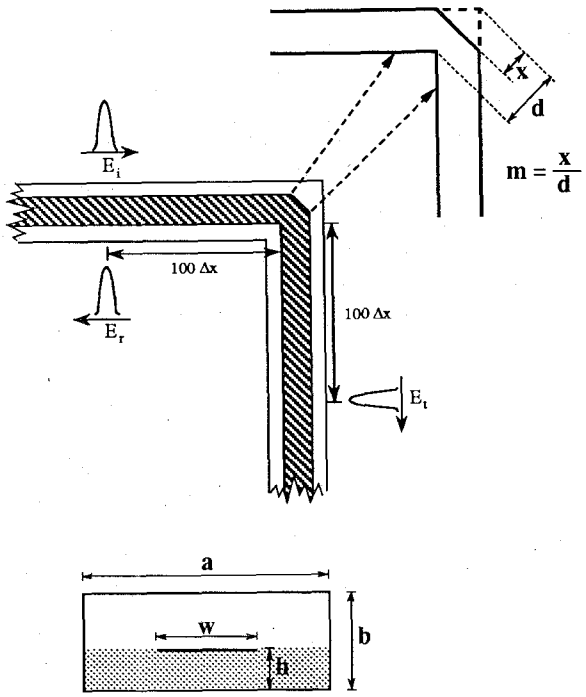

Fig. 1. The enclosed microstrip with right-angle bend. (a) Top view and detail of the mitered bend. (b) Cross-sectional view.

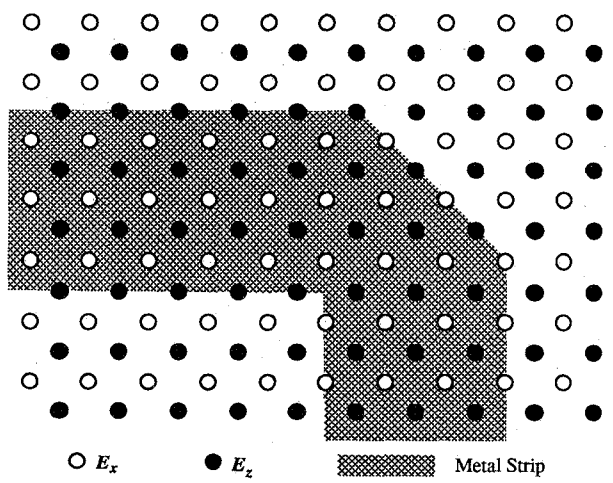

Fig. 2. Detail of the E-field nodes defining the metal strip.

In order to adequately define the bend and miter for the computer algorithm, this structure is first discretized into a three-dimensional finite difference mesh. Fig. 2 shows how electric wall boundary conditions are applied to individual nodes in order to define the metal strip. The fineness of the mesh, Δx, is chosen such that it is one tenth the length of the shortest wavelength of interest. Once the fineness of the mesh is given, the time step for iteration, Δt, is chosen to satisfy the Courant stability criterion [2].

Due to the dispersive nature of the microstrip and the complicated dielectric/metal/air boundary, conventional absorbing boundary conditions are avoided. Instead, a simple solution to this problem which saves some computer time and memory is to begin calculations on a short structure and to adaptively increase the structure length as a wave expands. The driving condition is enforced at what starts as the left edge of the FDTD grid, so that only an incident wave traveling to the right is produced. If the driving condition were left turned on while the grid expanded, then an incident wave traveling to the left would also be produced. This problem is avoided first by using an incident pulse of short duration and then by removing the driving condition when the grid begins to expand.

The incident pulse is a Gaussian pulse of short enough duration such that the driving condition is imposed on the structure for only the first few time steps. The time history of the reflected and transmitted waves is recorded. These data are then fast-Fourier-transformed and normalized with respect to the incident wave spectrum to obtain S_{11} and S_{21} as a function of frequency. The S_{11} and S_{21} phase references are chosen to be at the inner corner of the bend.

III. Results and Discussions

The microstrip line to be modeled was designed to be 50 Ω on a 3M substrate ($\epsilon_r = 2.5$). This design resulted in the following parameter values:

$$w = 2.31 \text{ mm} \qquad h = 0.84 \text{ mm}$$
$$\Delta x = 0.2096 \text{ mm} \qquad \Delta t = 0.4 \text{ ps}.$$

The cross section of the microstrip structure was first discretized into a 23×9 finite difference mesh. The length of the microstrip would begin at 2 cm and grow to about 17 cm by the end of the iterating process. The metal strip was 11 nodes wide, and this width enables the relative size of the cut, m, to be varied from 0 to 1 by increments of $1/22$.

The FDTD method was first run for the no-cut case. Fig. 3(a) shows the incident pulse which then propagated towards the right-angle bend and resulted in a reflected pulse (Fig. 3(b)) and a transmitted pulse (Fig. 3(c)). In order to calculate the proper phases of the S parameters, the propagation constant was obtained by observing the phase difference between two incident pulses separated by a known distance. This propagation constant is plotted against frequency in Fig. 4(a) along with the free-space propagation constant and the dielectric propagation constant. The dip in the propagation constant at about 27 GHz corresponds approximately to the first hybrid cutoff mode of the metal box enclosing the strip. The effective permittivity was computed directly from the propagation constant and is shown in Fig. 4(b) for three different values of box height ($b = 2h$, $3h$, and $4h$) and compared to a curve-fitted formula derived for the open microstrip case [18]. A change from $b = 2h$ to $b = 3h$ resulted in a sharp increase in effective permittivity, but the change then from $b = 3h$ to $b = 4h$ resulted in little change in the effective permittivity. This suggests that the box height at $b = 3h$ is large enough to not significantly affect the dispersion characteristics of the microstrip. The width of the box, a, appears to affect the propagation constant less than the height of the box, b. The effective permittivity is not significantly altered when the width of the box is changed from $a = 2w$ to $3w$, except for the shift in the cutoff frequency of the first hybrid mode. The characteristic

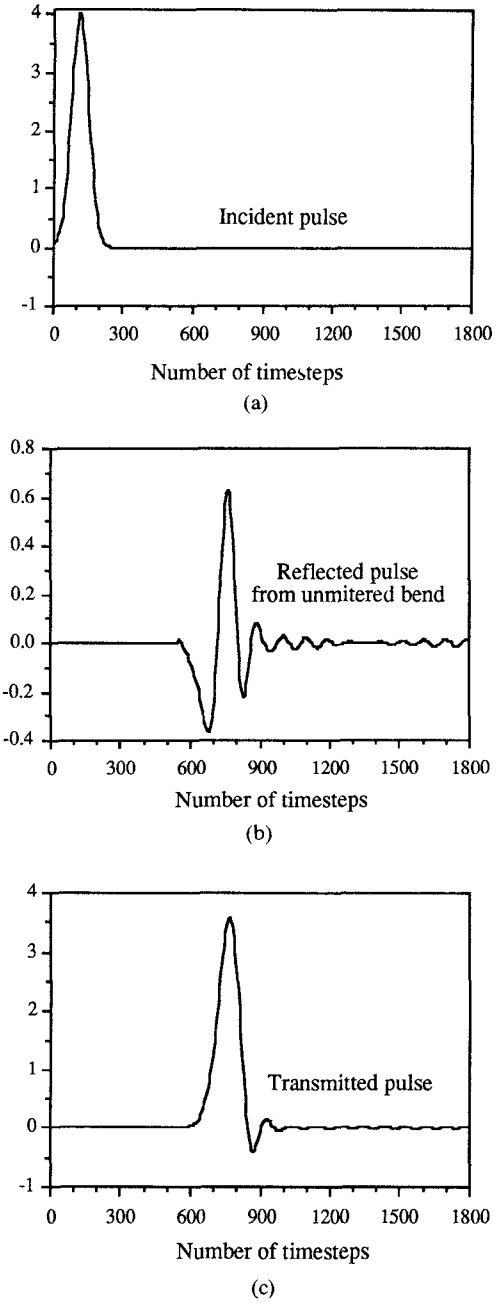

Fig. 3. Time histories for (a) the incident pulse, (b) the reflected pulse from the unmitered bend, and (c) the transmitted pulse for the unmitered bend.

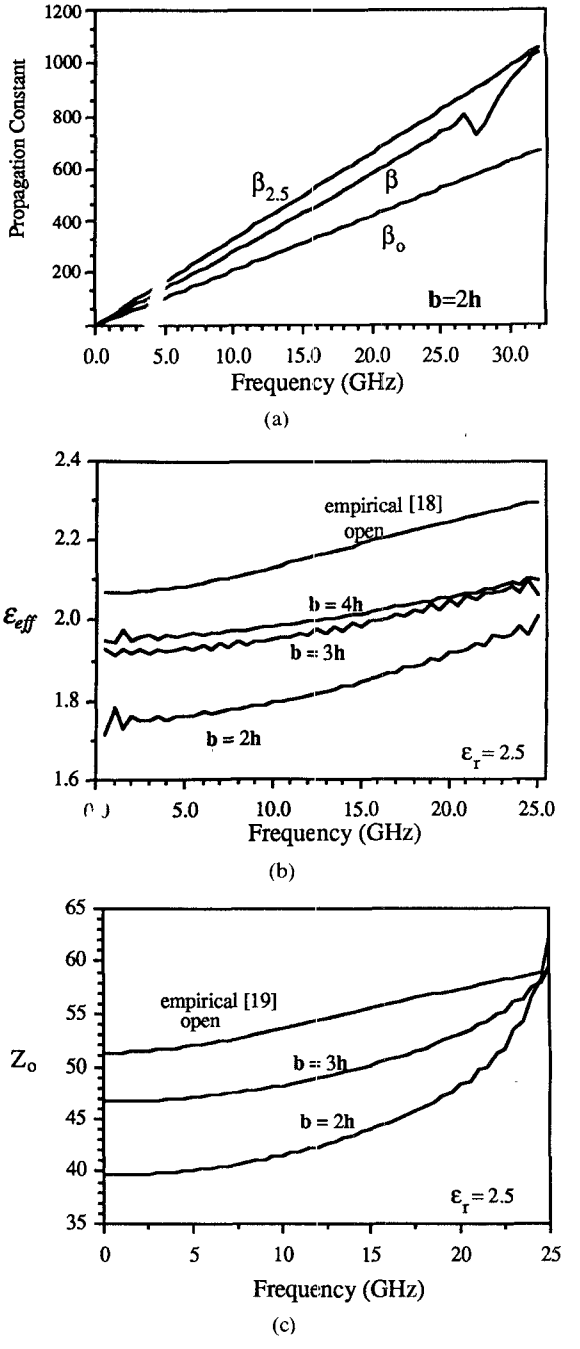

Fig. 4. Uniform microstrip characteristics calculated by the FDTD as compared with curve-fitted data for $\epsilon_r = 2.5$: (a) propagation constant; (b) effective dielectric constant; and (c) characteristic impedance.

impedances of the microstrip calculated by the FDTD method for two different box heights are compared in Fig. 4(c) with a curve-fitted formula for the open microstrip case [19]. An increase in b appears to move the characteristic impedance as well as the propagation constant closer to the open microstrip characteristic impedance. Bahl [20] reported similar effects of the enclosure upon the effective dielectric constant and the characteristic impedance of microstrip.

With the propagation constant in hand, the S parameters for the right-angle bend are completely determined. Both the magnitude and the phase of S_{11} and S_{21} for the no-cut case are shown in Fig. 5. Since the microstrip is enclosed, no radiation can occur, so the energy conservation criterion $|S_{11}|^2 + |S_{21}|^2 = 1$ was checked and found to be satisfied at all frequencies up to the cutoff frequency of the first higher order hybrid mode.

Mehran computed, via a waveguide model in conjunction with a two-dimensional mode-matching technique [10], a value of $|S_{11}| \approx 0.41$ which, when scaled in frequency to relate to the size of the microstrip modeled by the FDTD method, corresponds to $|S_{11}| \approx 0.30$ at 13 GHz. This discrepancy is probably due to the ambiguous definition of the "effective width" within the discontinuity region when analyzing the bend through the waveguide model.

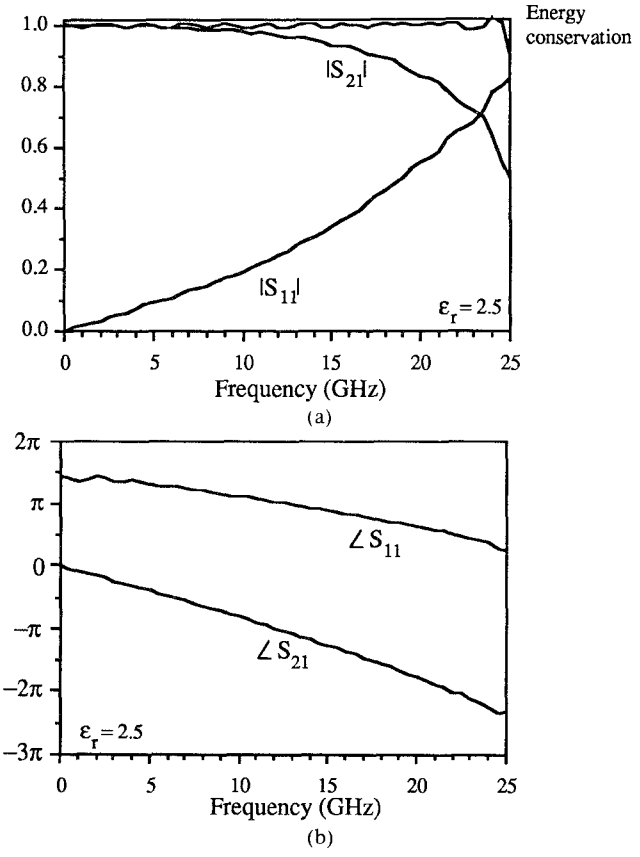

Fig 5. S parameters for the no-cut case: (a) magnitude; (b) phase.

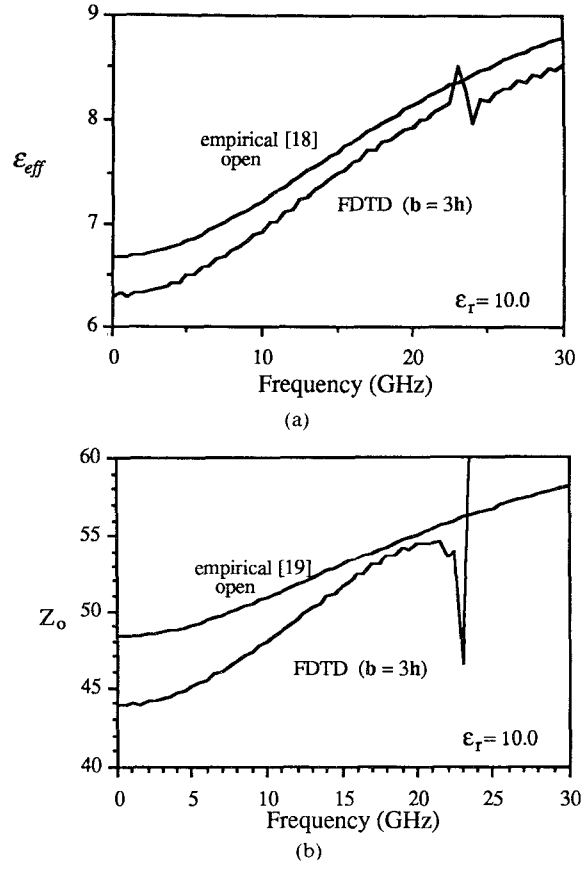

Fig. 6. Uniform microstrip characteristics calculated by the FDTD as compared with curve-fitted data for $\epsilon_r = 10.0$: (a) effective dielectric constant; (b) characteristic impedance.

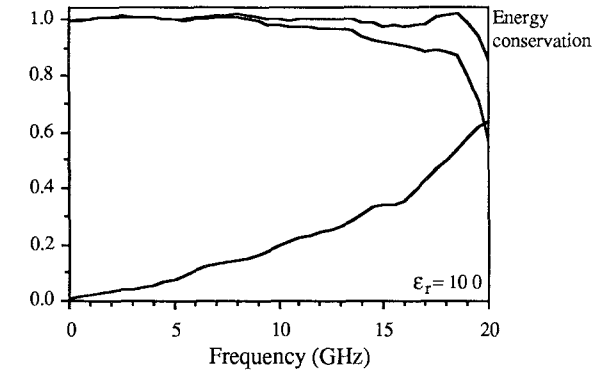

Fig 7. Magnitude of the S parameter for $\epsilon_r = 10.0$ without a miter.

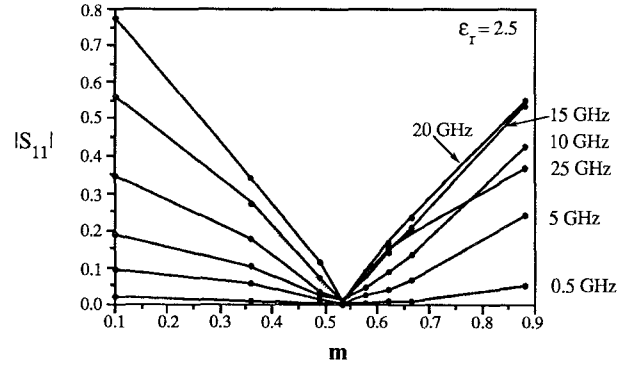

Fig 8. Magnitude of S_{11} versus cut size for $\epsilon_r = 2.5$

A second high-dielectric microstrip line to be modeled was designed to be 50 Ω on alumina substrate ($\epsilon_r = 10.0$) using the same values of h, Δx, and Δt as for the $\epsilon_r = 2.5$ case. This design resulted in $w = h = 0.84$ mm. The effective dielectric constant and the characteristic impedance were calculated and compared to curve-fitted data in Fig. 6. The effect of the enclosure of the box upon the effective dielectric constant appears less noticeable in the high-dielectric-substrate case than in the $\epsilon_r = 2.5$ case. Fig. 7 is a plot of the magnitudes of S_{11} and S_{21} for the high-dielectric case.

The cut size, m, was then varied to determine the optimal cut for the $\epsilon_r = 2.5$ case. Fig. 8 is a plot of S_{11} versus m. A broad-band optimal cut exists at $m = 0.53$. The time history of the reflected pulse for the optimal cut is shown in Fig. 9. The reflected pulse is barely noticeable for the optimal miter geometry. This optimal cut and six others for different width-to-height ratios and for substrates with high and low dielectric constants are compared with an empirical formula derived from measurement of open microstrip bends [15] in Fig. 10. The agreement is very good.

Finally, $|S_{11}|$ was checked against two different values of box height. $|S_{11}|$ for the no-cut case is shown in Fig. 11 for $b = 2h$, $3h$, and $4h$. The effect of the increase in b is noticeable only at higher frequencies, and there is almost no change in $|S_{11}|$ for the increase from $b = 3h$ to $b = 4h$.

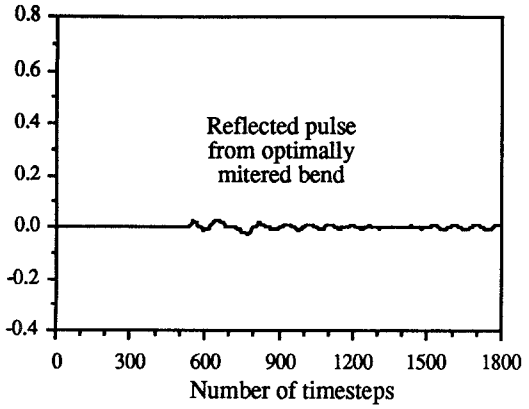

Fig. 9. Time history of the reflected pulse for the optimally mitered bend.

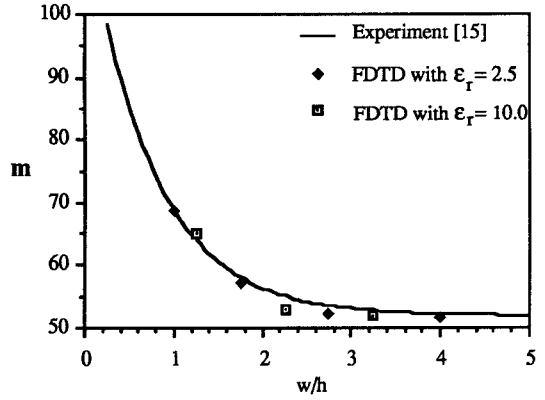

Fig. 10. FDTD optimal cut versus curve-fitting formula.

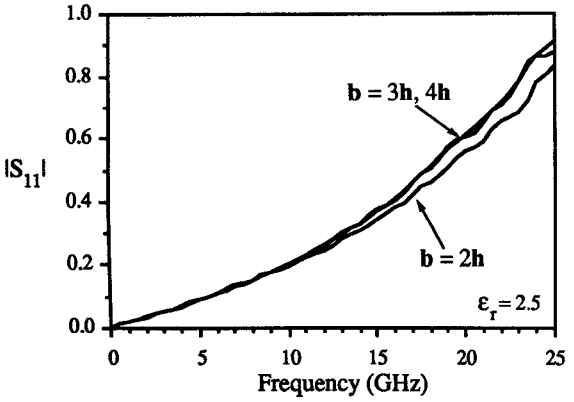

Fig. 11. Effects of change in box height on magnitude of S_{11}.

As a final check, the optimal cut for $b = 3h$ was computed and is the same size as the optimal cut for $b = 2h$.

IV. Conclusions

A microstrip with a right-angle bend has been simulated via the time-domain finite difference method. Electric walls were used to enclose the microstrip structure. Numerical results for the enclosed bend appear to agree well with experimental results for the open bend. Douville and James [15] noted that radiation associated with the bend is not important. Furthermore, the slight change in S parameters of the enclosed microstrip bend when the enclosing box is increased in height from $b = 3h$ to $b = 4h$ suggests that the FDTD results are close to results expected for the open microstrip bend. Finally, the FDTD method had equal success for both high- and low-dielectric materials.

References

[1] K. S. Yee, "Numerical solution of initial boundary value problems involving Maxwell's equations in isotropic media," *IEEE Trans. Antennas Propagat.*, vol. AP-14, pp. 302–307, May 1966.

[2] A. Taflove and M. E. Brodwin, "Numerical solution of steady-state electromagnetic scattering problems using the time-dependent Maxwell's equations," *IEEE Trans. Microwave Theory Tech.*, vol. MTT-23, pp. 623–630, Aug. 1975.

[3] W. K. Gwarek, "Analysis of an arbitrarily-shaped planar circuit—A time-domain approach," *IEEE Trans. Microwave Theory Tech.*, vol. MTT-33, pp. 1067–1072, Oct. 1985

[4] W. K. Gwarek, "Analysis of arbitrarily shaped two-dimensional microwave circuits by finite-difference time-domain method," *IEEE Trans. Microwave Theory Tech.*, vol. 36, pp. 738–744, Apr. 1988.

[5] X. Zhang, J. Fang, K. K. Mei, and Y. Liu, "Calculations of the dispersive characteristics of microstrips by the time-domain finite difference method," *IEEE Trans. Microwave Theory Tech.*, vol. 36, pp. 263–267, Feb. 1988.

[6] X. Zhang and K. K. Mei, "Time-domain finite difference approach to the calculation of the frequency-dependent characteristics of microstrip discontinuities," *IEEE Trans. Microwave Theory Tech.*, vol. 36, pp. 1775–1787, Dec. 1988.

[7] P. Silvester and P. Benedek, "Microstrip discontinuity capacitances for right-angle bends, T-junctions, and crossings," *IEEE Trans. Microwave Theory Tech.*, vol. MTT-21, pp. 341–346, May 1973.

[8] G. Kompa, "*S*-matrix computation of microstrip discontinuities with a planar waveguide model," *Arch. Elek. Übertragung.*, vol. 30, pp. 58–64, 1975.

[9] W. Menzel and I. Wolff, "A method for calculating the frequency-dependent properties of microstrip discontinuities," *IEEE Trans. Microwave Theory Tech.*, vol. MTT-25, pp. 107–112, Feb. 1977.

[10] R. Mehran, "Calculation of microstrip bends and Y-junctions with arbitrary angle," *IEEE Trans. Microwave Theory Tech.*, vol. MTT-26, pp. 400–405, June 1978.

[11] R. Chadha and K. C. Gupta, "Compensation of discontinuities in planar transmission lines," *IEEE Trans. Microwave Theory Tech.*, vol. MTT-30, pp. 2151–2156, Dec. 1982.

[12] N. Yoshida and I. Fukai, "Transient analysis of a stripline having a corner in three-dimensional space," *IEEE Trans. Microwave Theory Tech.*, vol. MTT-32, pp. 491–498, May 1984.

[13] G. Mur, "Absorbing boundary conditions for the finite-difference approximation of the time-domain electromagnetic-field equations," *IEEE Trans. Electromagn. Compat.*, vol. EMC-23, pp. 377–382, Nov. 1981.

[14] J. Fang and K. K. Mei, "A super-absorbing boundary algorithm for solving electromagnetic problems by time-domain finite-difference method," in *IEEE AP-S Int. Symp. Dig.* (Syracuse, NY), June 1988, pp. 472–475.

[15] R. J. P. Douville and D. S. James, "Experimental study of symmetric microstrip bends and their compensation," *IEEE Trans. Microwave Theory Tech.*, vol. MTT-26, pp. 175–182, Mar. 1978.

[16] N. Marcuvitz, *Waveguide Handbook* (Radiation Laboratory Series, vol. 10). New York: McGraw-Hill, 1951

[17] J. J. Campbell and W. R. Jones, "Symmetrically truncated right-angle corners in parallel-plate and rectangular waveguide," *IEEE Trans. Microwave Theory Tech.*, vol. MTT-16, pp. 517–529, Aug. 1968.

[18] R. P. Owens, "Accurate analytical determination of quasi-static microstrip line parameters," *Radio and Electron. Eng.*, vol. 46, pp. 360–364, 1976.

[19] B. Bianco *et al.*, "Frequency dependence of microstrip parameters," *Alta Frequenza*, vol. 43, pp. 413–416, 1974.

[20] I. J. Bahl, "Easy and exact methods for shielded microstrip design," *Microwaves*, vol. 17, Dec. 1974.

✠

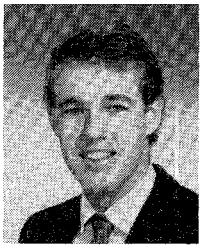

John Moore (S'84) was born in Bethesda, MD, on December 7, 1966. He received the B.S. and M.S. degrees in electrical engineering from the University of Texas at Austin in 1988 and 1989, respectively. He is currently working toward the Ph.D. degree, also at the University of Texas.

During the summers of 1985 and 1986 he was a research assistant at the Uniformed Services University of the Health Sciences in Bethesda, MD. In the summer of 1987 he was awarded the Shulz Memorial Fellowship, through which he worked at the Electromagnetics Laboratory of the University of Illinois at Urbana/Champaign. His main research interest is in time-domain solutions to electromagnetics problems.

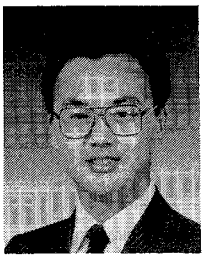

Hao Ling (S'83–M'86) was born in Taichung, Taiwan, on September 26, 1959. He received the B.S. degrees in electrical engineering and physics from the Massachusetts Institute of Technology in 1982 and the M.S. and Ph.D. degrees in electrical engineering from the University of Illinois at Urbana-Champaign in 1983 and 1986, respectively.

In 1982, he joined the IBM Thomas J. Watson Research Center, Yorktown Heights, NY, where he conducted low-temperature experiments in the Josephson Department. While in graduate school at the University of Illinois, he held a research assistantship in the Electromagnetics Laboratory as well as a Schlumberger Fellowship. In 1986, he joined the Department of Electrical and Computer Engineering, the University of Texas at Austin, as an Assistant Professor. He participated in the Summer Visiting Faculty Program in 1987 at the Lawrence Livermore National Laboratory. His current research interests include radar cross section analysis of partially open cavities and the characterization of the microstrip discontinuities.

Dr. Ling is a recipient of the 1987 National Science Foundation Presidential Young Investigator Award.